The Extracellular Matrix as a Target for Biophysical and Molecular Magnetic Resonance Imaging

Chapter · February 2018

DOI: 10.1007/978-3-319-65924-4_6

4 authors, including:

Angela Ariza de Schellenberger
Charité Universitätsmedizin Berlin
30 PUBLICATIONS **79** CITATIONS
SEE PROFILE

Judith Bergs
Charité Universitätsmedizin Berlin
28 PUBLICATIONS **311** CITATIONS
SEE PROFILE

Matthias Taupitz
Charité Universitätsmedizin Berlin
348 PUBLICATIONS **8,272** CITATIONS
SEE PROFILE

The Extracellular Matrix as a Target for Biophysical and Molecular Magnetic Resonance Imaging

6

Angela Ariza de Schellenberger, Judith Bergs, Ingolf Sack, and Matthias Taupitz

Abstract

All tissues and organs are composed of cells and extracellular matrix (ECM). The components of the ECM have important functional and structural roles in tissues. On the one hand, the ECM often dominates the biomechanical properties of soft tissues and provides mechanical support to the tissue. On the other hand, ECM components maintain tissue homeostasis, pH, and hydration of the micromilieu and, via signal transduction, also play a key role in ECM-cell interactions which in turn control cell migration, differentiation, growth, and death. Inflammation, fibrosis, tumor invasion, and injury are associated with the transition of the ECM from homeostasis to remodeling which can dramatically alter the biochemical and biomechanical properties of ECM components. Hence, it is possible to detect and characterize disease by sensing biochemical and biomechanical changes of the ECM when appropriate imaging methods are used. This chapter discusses ECM-specific magnetic resonance imaging (MRI) based on contrast agents and elastography from a clinical radiological perspective in a variety of diseases including atherosclerosis, cardiomyopathy, inflammation, and liver fibrosis.

6.1 Introduction

All tissues and organs of vertebrates are composed of cellular and noncellular components, and the latter are often collectively referred to as *extracellular matrix* (ECM). Connective tissues of skin, cartilage, vessel walls, and intervertebral discs are rich in ECM and have the best-characterized ECM. As early as 1929, the

A. Ariza de Schellenberger • J. Bergs • I. Sack • M. Taupitz (✉)
Department of Radiology, Charité – Universitätsmedizin Berlin, Berlin, Germany
e-mail: Matthias.Taupitz@charite.de

I. Sack, T. Schaeffter (eds.), *Quantification of Biophysical Parameters in Medical Imaging*, https://doi.org/10.1007/978-3-319-65924-4_6

adhesive and sticky properties of cells were linked to their self-produced ECM [1]. Initially, the ECM was thought to be a structural element of tissues only, but its active role in cell differentiation, development, cell migration and tissue homeostasis is increasingly recognized [2, 3].

While there is an overwhelming diversity of structures and forms of biological tissues, the variety in the chemical ECM composition is fairly small. Essentially, fibrous proteins, glycoproteins (GP), proteoglycans (PG), glycosaminoglycans (GAGs), salts, and water (approx. 80% of the ECM wet weight) make up the ECM and thereby determine the biophysical and chemical environment of cells [3].

The biophysical properties of many tissues are largely governed by their ECM components and their interactions. The stroma of the eye's cornea, for example, consists of regularly arranged collagen fibers that withstand large tensile forces giving rise to a large elastic modulus greater than 50 MPa [4]. In contrast, the vitreous body of the eye is mainly made up of hydrated polysaccharide gels immersed by sparse collagen fibers, resulting in an elastic modulus below 2 Pa [4]. This huge difference in elasticity on the order of 10^6 illustrates the crucial role of ECM structures for the mechanical properties of tissues. The components of the ECM are produced by tissue-resident cells and secreted into the ECM. Once the molecules have been secreted, they aggregate within the existing matrix to support cellular viability [3]. This insight led to the once predominant view of cells as the key components of tissues. Many discoveries in recent years have led to a reappraisal, pointing to the importance of the ECM for many vital processes [5–8]. The ECM provides structural support, separates cells at tissue interfaces, and provides cellular signaling through cell-matrix connections such as focal adhesions. The latter influence cell morphology, movement, functions, and even cell fate. Cells and the ECM form a symbiotic unit that defines both the physiological functions and macroscopic properties of a biological tissue. The ECM is highly dynamic: chemical and structural changes occur during embryonic development and tissue homeostasis and can also be induced by pathophysiological stimuli and injury. These insights motivate research in the field of biomedical imaging aimed at identifying ECM-specific targets. The prospect of developing biophysical and molecular probes for ECM imaging offers a promising direction of molecular medical imaging in parallel to the development of cell-specific imaging probes. In this chapter, we will review the foundations of ECM-specific medical imaging with a focus on clinical magnetic resonance imaging (MRI). Before continuing we give a brief overview of the composition and constituents of the ECM in soft tissues of vertebrates.

6.2 Composition of the ECM

The ECM is a mesh-like structure composed of the *basement membrane* (BM) and the *interstitial matrix* (Fig. 6.1). The BM is a highly cross-linked constituent of the ECM that is composed of sheetlike depositions secreted by epithelial cells and localized between the epithelial cells and the underlying connective tissue. The BM separates the epithelium from the stroma of any given tissue. The BM is always in

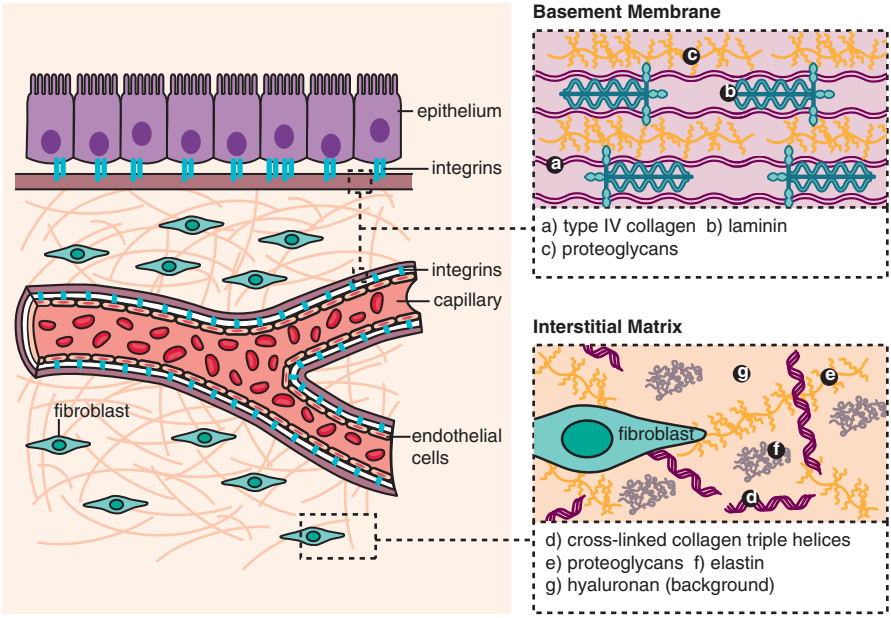

Fig. 6.1 Diagram of the histologic structure of the ECM. The basic subdivision of the ECM into basement membrane and interstitial matrix is shown along with major structural components (collagen and elastin) as well as the background matrix made up of proteoglycans and HA

contact with the cells, provides structural support, divides tissues into compartments, and regulates cell behavior [9, 10]. Overall, about 50 proteins are known to make up the BM of which approx. 50% are of the collagen type (especially type IV collagen). The BM is formed by three layers: the lamina densa, the lamina lucida, and a network of reticular collagen type III [1]. The lamina densa (*collagen IV*, perlecan, heparan sulfate proteoglycans (*HSPG*)) and the lamina lucida (*laminin*, integrins entactin and dystroglycans) form networks connected by nidogen (entactin), which is also known to bind proteoglycans and fibulins [11]. The variability of the BM in different tissues is mainly due to the ratio of type IV collagen, laminin, and HSPG [9, 12]. Collagen IV fibers aggregate into a network and provide the scaffold of a matrix with laminin as the central part. This matrix is essential for cells and other BM components that interact with each other such as perlecan, nidogen (entactin), fibulin, and collagen XVIII [13–18]. The laminin family of ECM glycoproteins is the major noncollagenous constituent of the BM and is also involved in cellular processes such as differentiation, migration, signaling, and tumor invasion. Laminins are composed of three nonidentical chains that combined form different heterotrimeric laminin isoforms, e.g., laminin 1 is a $\alpha 1\beta 1\gamma 1$ heterotrimer [19]. Laminin incorporation into the ECM is dependent on its interactions with other ECM molecules such as collagen IV, nidogen, fibulins, and other laminin molecules. The major cell surface receptors for laminins are integrins, which have a high binding specificity for different cell types. Laminin function is altered by

posttranslational modifications, i.e., covalent or enzymatic modifications during or after protein synthesis. Therefore, the detection of both laminin and integrin receptors is required in order to study cellular function [20–23]. The components of the BM can be modified by structural or functional changes, e.g., as required for blood vessel formation (neoangiogenesis) and cancer progression [9, 23–25]. Furthermore, fibronectin attaches cells to different ECM components and forms part of the connective tissue that is the ECM at interfaces and organ boundaries.

The *interstitial* or *intercellular space* is the other major ECM compartment next to the BM. Structural proteins such as collagens are mainly immersed in the interstitial space. Collagens are the most abundant proteins of the ECM and account for roughly 30% of the total mass of proteins in the body. There are over 28 different types of collagen fibrils. Collagen types I, II, and III are the most abundant, and collagen I constitutes nearly 90% of all the collagen in the human body. Collagens are mostly synthesized by fibroblasts, but epithelial cells also contribute to the synthesis of some collagens in the ECM. Skin, cartilage, tendons, and ligaments are particularly rich in collagens, which form mechanical networks and supportive structures that determine the shear modulus and limit the extensibility of these tissues. In contrast, tissues with high stretching or bending capacity are rich in elastic fibers characterized by cross-linked elastin interspersed with fibrillins. Elastin is particularly abundant in the walls of large arteries, skin, and lungs, influencing the linear tensile elastic properties of these tissues.

The major volume-occupying components of interstitial spaces are glycosaminoglycan chains (GAGs) attached to the core proteins, forming proteoglycans (PGs). PGs are macromolecules consisting of a core protein heavily glycosylated by one or more covalently bound carbohydrate chains. The biophysical function of PGs depends on their bound GAGs such as keratan sulfate (KS) and dermatan sulfate (DS) chains, whose strong negative charge allows them to bind large amounts of water and to fill most of the interstitial space as hydrated gels [2] (see Fig. 6.2). Interstitial PGs can interact with collagens and thereby also influence the structural organization of tissues. Because of the incompressibility of water, hydrated proteoglycan gels constitute the main mechanical support of tissues against compressive forces, whereas fibrillar proteins such as collagen and elastin resist stretching forces [3]. PGs, such as aggrecan, provide lubricating function to joints and structural integrity to cells and allow cell migration and diffusion of cell factors essential for cell communication [26, 27]. PGs are also involved in the organization of BM structures and thereby influence epithelial cell migration, proliferation, and differentiation. Thus, many biological functions involved in tissue development and homeostasis are mediated by specific binding of GAGs to macromolecules, mostly proteins. For example, PGs can accumulate in secretory vesicles, maintain proteases in their active state, and regulate biological activities after secretion, such as coagulation, host defense, and wound repair. Specifically, blood coagulation is controlled by GAGs such as heparin and, to a lesser extent, by heparan sulfate (HS) binding antithrombin III. When no binding proteases (thrombin, factors IVa and XIa) are present, thrombus formation is inactivated or slowed down, and blood coagulation is distorted [28]. PGs can also bind cytokines, chemokines, growth factors, and

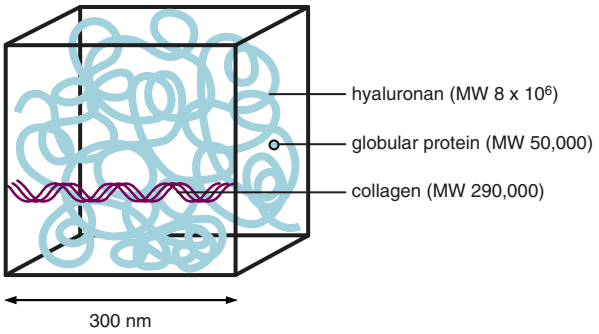

Fig. 6.2 Illustration of the relative volumes occupied by collagen, globular proteins, and a single hydrated HA molecule. MW denotes the relative molecular weight

morphogens, protecting them against proteolysis. These interactions involve a reservoir of regulatory factors that can be released by selective ECM degradation. For example, PGs can bind growth factors from the fibroblast growth factor (FGF) family, which also bind GAGs such as heparin or HS trapped inside the ECM. These GAGs can alter the conformation of this complex and distort normal release of FGF, thereby influencing cell proliferation or activation [29, 30].

In general, biological PG function depends on the interaction of GAG chains with different protein ligands, e.g., integrins and other cell receptors assisting in cell attachment, cell interaction, and cell migration [31, 32].

6.2.1 Glycosaminoglycans (GAGs) in the ECM

GAGs consist of linear polysaccharide chains composed of repeating disaccharide units, which consist of a hexose or hexuronic acid (or a galactose for keratan sulfate) and a hexosamine [28, 33]. They are highly hydrophilic and can adopt extended conformations essential for hydrogel formation. Therefore, GAGs in connective tissue, while constituting less than 10% of the structural proteins, occupy most of the extracellular space (Fig. 6.2) [3]. GAGs can be subdivided into sulfated GAGs (chondroitin sulfate (CS), dermatan sulfate (DS), keratan sulfate (KS), heparan sulfate (HS), and heparin)) and nonsulfated GAGs (hyaluronan, HA). Only sulfated GAGs are covalently bound to proteins, forming a total of 43 different types of proteoglycans [34]. GAGs are primarily located on cell surfaces and in the ECM but are also found in secretory vesicles in some types of cells. The distribution of GAGs differs with the type of tissue: while HA is a major component of the ECM of cartilage, CS is bound to the cell surface, e.g., in the brain and cartilage [35–37]. DS is present in skin and the nervous system, often bound to CS, while KS is more abundant in cartilage and cornea [37–40]. The function of GAGs depends on the protein with which they interact and the orientation and nature of GAG-bound sulfate groups. In general, the properties of GAGs tend to dominate the chemical properties of PG. GAGs can influence physiological processes, such as development, angiogenesis, and innate immunity, but also cancer and neurodegenerative diseases [38–43]. HS is the most common GAG and can sequester growth factors in the ECM.

It is involved in inflammatory processes and malignant processes such as invasive growth and metastatic spread [29] as well as other pathophysiological and physiological processes [29, 44–46]. HA is a unique GAG because it does not contain any sulfate group and has not been found to be covalently bound to a core protein to form PG [34, 47]. Instead, it is often noncovalently linked to PG and can immobilize large amounts of water. Due to the large amount of bound water, hydrogels formed by GAGs are nearly incompressible, which makes them ideal for lubrication in the joints. For instance, the unique biophysical properties of HA are fundamental for the mechanical functioning of synovial fluid or the resistance of connective tissues to compressive forces [48]. HA is predominantly necessary to maintain indirect interaction with other components of the ECM such as fibronectin, laminin, collagen, and PG. Together with its cellular receptor (CD44), HA plays an essential role in cell migration, tissue development, and inflammation and is often used in regenerative medicine [49–53]. One special feature of GAGs is their structural heterogeneity, mostly due to chemical modifications during and after synthesis. This makes the development of analytical techniques for GAGs (glycosaminoglycomics) challenging [33].

Different physiological activities arise from the variability of GAGs in the amount of negative charges and the presence of carboxylate and sulfate groups, which can bind cationic ions. Since GAGs are virtually polyanionic polymers, Ando et al. postulated that GAGs, especially in their sulfated forms, are similar to ion-exchange resins [54]. One special property of GAGs is that, with increasing disease severity, they are modified by corresponding enzymes, e.g., resulting in enhanced sulfation [55]. The degree of GAG sulfation in several inherited disorders and pathologies, as well as inflammation-involved sulfated GAGs, have been described [28, 45, 46, 56].

In normal tissue, GAGs are predominantly organized with the complexing groups forming hydrogen bonds [57], but in pathological processes, ranging from inflammation to tumor invasion, an increase in one or more GAG components takes place, and potentially complex-forming groups become exposed [55, 58–62]. It has been demonstrated in models of chemically induced tumors that characteristic changes in the ECM, especially alterations in GAG components, already take place at the preneoplastic stage [63]. In patients with malignancy, the patterns of GAG composition have prognostic significance for the subsequent disease course, in particular with regard to the risk of recurrence and metastatic spread [64]. GAGs are also a major component of the glycocalyx-a paracellular matrix located on the surface of endothelial cells. In fact, the endothelium is negatively charged due to the high proportion of highly sulfated GAGs included in the glycocalyx [65]. The glycocalyx contributes to the barrier function of the epithelium between the vascular and interstitial compartments and regulates the transport by diffusion of low-molecular-weight substances, the controlled transport of macromolecules and particles, and the passage of cells. It has been shown that an increase in the shear stress on vascular endothelium leads to a change in the GAG composition of the glycocalyx with an increase in HA [66], which provides further evidence for the central role of mechanical signal transduction between cells and their ECM. Higher levels of shear stress have been reported to be associated with an increase in GAG sulfation [67]. It is known that the glycocalyx has a function in

mechanotransduction—a mechanism by which cells sense mechanical stimuli such as hemodynamic changes, e.g., blood flow velocity and pressure, and translate them into cellular responses, e.g., enhanced NO synthesis [68]. Pathological tissue changes, especially inflammation, are associated with an alteration in the glycocalyx of the local vascular endothelium, which affects the adhesion and transendothelial transport of endogenous and exogenous low-molecular-weight and macromolecular substances [65, 69].

Another observation worth mentioning in the context of GAG function is that carboxyl and sulfate groups not only bind to physiologically occurring ions such as K^+, Na^+, Ca^{2+}, Zn^{2+}, and Cu^{2+} but also have high affinity to lanthanide ions like Gd^{3+} and La^{3+} [70–72]. This property offers a target for ECM-directed imaging that can be exploited by targeting GAG components of the ECM using, for example, cationic ions or molecules that function as signal-generating moieties in the imaging modality used. On the other hand, GAGs may contribute to the retention of Gd after intravenous injection of Gd-based contrast media, as frequently used in clinical routine. The exact mechanisms for tissue retention of Gd after intravenous injection of Gd-based contrast media are still not fully understood [73–81].

Glossary

Glycosaminoglycans (GAGs): Long, negatively charged, linear chains of disaccharide repeats. Major GAGs include HS (component of basement membrane), CS (cartilage and neural ECM), DS (skin, blood vessels, tendons, lungs), HA, and KS (cornea, cartilage, bone).

Proteoglycans (PG): Heavily glycosylated proteins formed by GAG chains covalently linked to a core protein. Proteoglycans provide hydration and compressive resistance to ECM and hold numerous other biological functions including support of cell signaling, proliferation and migration, wound repair by binding of growth factors, cytokines, and ECM proteins.

Fibrous proteins: Also called scleroproteins, these proteins are characterized by their insolubility and their fibrous structure and, among others, include collagen, elastin, fibronectin, and laminin. These proteins are produced by fibroblasts and are released in a precursor form; their subsequent incorporation into the ECM is guided by fibroblasts according to the functional needs of the resident tissue.

Fibronectin: High-molecular-weight multi-domain protein with binding capacities to cell surfaces through integrins and other biologically important molecules such as collagen and HSPGs. Fibronectin plays a major role in cell adhesion, growth, migration, and differentiation and is involved in wound healing.

Laminins: Glycoproteins that constitute the structural scaffolding of all basement membranes. Laminins bind integrins, dystroglycans, and numerous other receptors. These interactions are critical for cell differentiation, movement, cell shape, and survival.

Integrins: Transmembrane linkers that mediate interactions between the ECM and intracellular cytoskeleton or intercellular interactions. Therefore, integrins can interact with fibronectin (in the ECM) and actin (in the cytoskeleton of cells) and trigger intracellular signal transduction pathways via protein kinases (focal adhesion kinase and integrin-linked kinase), which are essential for cell migration, growth, and survival.

Glycocalyx: A glycoprotein-polysaccharide that forms a filamentous coating on the apical surface of some bacteria and interspersed among cells of the digestive tract microvilli, as well as in vascular endothelial cells. The glycocalyx also consists of a wide range of enzymes and proteins. The glycocalyx enables cells to recognize each other, helping the body to identify healthy cells and transplanted tissues or invading microorganisms. In addition, it also guides cellular movement during embryogenesis. In endothelial vascular tissue, the glycocalyx plays a major role in maintenance of plasma and vessel wall homeostasis.

Collagen: Main structural protein in mammals constituting approximately 30% of all proteins in the body. It has the capacity to bind to cell surface receptors, proteins, GAGs, and nucleic acids. The most abundant collagens are type I (component of, e.g., organs, bone, and skin) and type III (component of reticular fibers). The fibrillar collagen types I and III self-assemble into hierarchical structures are capable of withstanding tensile forces and provide mechanical integrity to the interstitial matrix. The nonfibrillar collagen type IV is a major component of the basement membrane that forms loose, sheetlike structures, which influence cell differentiation, migration, and adhesion and angiogenesis.

Elastin: Fibrous protein which is, to a major portion, responsible for the elastic (mechanical energy restoring) properties of soft biological tissues. Elastin is composed of cross-linked tropoelastin, a 60–70 kDa monomeric protein with hydrophobic and lysine-containing crosslinking domains [82]. The elastic properties of elastin networks are thought to be due to their random coil structures of cross-linked elastin molecules which allow the network to stretch and recoil like a rubber band [3].

6.3 Alteration of the ECM in Disease

The potential role of ECM-targeted medical imaging can be discussed for a variety of diseases with high clinical relevance. Therefore, the focus will be on the following conditions:

- Atherosclerosis and aortic aneurysm
- Cardiomyopathy
- Neuroinflammation
- Inflammatory bowel disease
- Liver fibrosis

The following sections present a brief overview of the current state of knowledge on the most important components of the ECM involved in these disease entities.

6.3.1 Atherosclerosis and Aortic Aneurysm

The development and progression of atherosclerotic plaques are accompanied by significant changes in the composition of the ECM of the vascular wall, eventually leading to plaque rupture. The chondroitin sulfate proteoglycan (CS-PG) versican appears to play a key role in this process. Versican is increased already at an early stage in the development of atherosclerotic plaques [83, 84]. Versican interacts with HA, the content of which also increases in the atherosclerotic vascular wall. Versican plays an important role in the regulation of plaque progression. It binds lipoproteins and leads to their accumulation in the affected vascular wall dependent on the length of the CS chains [53, 83]. In addition to versican, other proteoglycans are involved in atherosclerosis including biglycan, decorin, and perlecan. The content of elastin and collagen in the vessel wall decreases as atherosclerotic wall lesions become destabilized, while an increase in elastin and collagen indicates stabilization of the diseased vessel wall [85]. Type I, II, IV, V, and VI collagens are involved in the process of plaque formation, depending on the stage of the plaque and its location in the vascular wall. Atherosclerotic plaques can be classified using the methods of Stary [86] and Virmani [87], which are based on staining the components of the plaque ECM by Movat's pentachrome stain. The vascular wall of aortic aneurysms shows an inflammatory component and is characterized by medial degeneration [88], marked mainly by a degradation of elastin and by unorganized deposition of collagen. Loss of elastin leads to dilatation of the vascular wall, and collagen depletion increases the risk of rupture. GAG accumulation in the vascular wall and the associated pathological changes in the biomechanical properties of the aortic wall are considered a major factor underlying dissection in aortic aneurysm [89].

6.3.2 Cardiomyopathy

Myocardial damage leads to remodeling, which includes increased formation of glycoproteins, proteoglycans, and GAGs for regulation of inflammation, fibrosis, and angiogenesis [90]. Furthermore, the pathological cascade in myocardial damage involves increased accumulation of collagen, eventually leading to dilated cardiomyopathy. With progressing fibrosis and scarring, the damaged myocardium reacts by local accumulation of chondroitin sulfate (CS) and dermatan sulfate (DS) [91, 92]. This process is accompanied by an increase in sulfation of these GAGs immediately after the damage has occurred [93].

6.3.3 Neuroinflammation

The ECM also plays a key role in the growth and structural development of the central nervous system, regulating interactions between cells including neurons,

glia, and inflammatory cells [7]. Normal aging of the brain is associated with a reduction of the CS-PG content of the ECM [94]. This change in the ECM alters the diffusion of small molecules and water, thereby altering the biochemical properties of CNS tissue and eventually the global biomechanical properties of the brain [95]. Sulfation of GAGs in inflammatory CNS pathologies and after mechanical tissue damage regulates cell migration as well as anti- and proinflammatory processes. For example, perivascular accumulation of HS alone or as a PG-component was found in MS lesions [96]. Dense networks of ECM components, i.e., CS- and DS-PGs and HA, have been observed in active MS lesions but not in chronic inactive MS lesions [97]. Local HA accumulation was already identified in early inflammatory demyelinating CNS lesions [98].

6.3.4 Inflammatory Bowel Disease

Marked ECM alterations also occur during the development of chronic inflammatory bowel diseases. In Crohn's disease, inflamed sections of the bowel wall have increased levels of HSPG, CS, and DS. As the disease progresses, the formation of collagen also increases, leading to fibrosis and changes in the biomechanical properties of the bowel wall [99]. Intestinal structures are more likely to occur as a clinical complication in Crohn's disease than in ulcerative colitis [100]. Roughly 30% of patients with Crohn's disease develop intestinal fibrosis with stenosis, but only 5% develop ulcerative colitis [101].

6.3.5 Liver Fibrosis and Cirrhosis

In the development of liver fibrosis and cirrhosis, the composition of the ECM becomes impaired at an early stage due to alterations in the synthesis and degradation of ECM components. The collagen content rises with the degree of fibrosis, resulting in an increase in tissue rigidity [8, 102–104]. A distinct increase in HA, CS, and DS has also been found in various models of liver damage and liver fibrosis [63, 105, 106].

Overall, inflammatory processes lead to a marked increase in the amount of ECM components as well as significant structural changes within the ECM—all of which affect the biochemical and biophysical properties of the tissue. Elastography, which is sensitive to mechanical tissue structures, has been validated as the most precise noninvasive biomarker for staging hepatic fibrosis [107]. However, it remains open which ECM components and cells contribute to the mechanical scaffold of liver tissue and how these structures change with different etiologies [108]. Since early structural changes in the liver do not impact overall hepatic function, blood biomarkers or functional breath tests are less accurate for the assessment of early fibrotic processes in the liver [104].

6.4 ECM-Specific Medical Imaging

In current clinical radiology, the majority of substances used for the enhancement of image contrast are unspecific. The contrast-enhancing agents used in clinical X-ray radiography, CT, or MRI are all based on iodinated or gadolinium-containing low-molecular-weight substances. Following intravenous injection, these agents are distributed in the intravascular and interstitial space, and a large proportion is rapidly eliminated via the kidneys. These clinical contrast agents enhance signal in regions where pathological processes are present in an unspecific manner. Unspecific pathological processes include inflammation, neovascularization, changes in local blood volume, altered permeability of the vessel wall, and increased volume of extracellular spaces. Noteworthy, the limited specificity of most contrast agents in clinical routine is the reason for their commercial success since the number of potential applications is high. Nevertheless, research groups worldwide attempt to target molecular structures at cell surfaces or metabolic processes by developing highly specific imaging probes [109]. Some very interesting disease-specific molecular imaging approaches using MRI, sonography, radionuclide imaging, and optical imaging were demonstrated to be experimentally feasible for detection of inflammatory [110–112], malignant [113–115], and degenerative processes [116–118]. However, except for radionuclide imaging, which is sensitive already at very low radionuclide concentrations (see Chap. 21), the translation of molecular probes into clinical use has been successful only in a very limited number of cases. The MRI contrast agent Primovist has been shown to enable hepatocyte-specific imaging [119, 120]. Another MRI contrast agent, Resovist, allows targeting of phagocytosing cells in liver neoplasms [121, 122]. In general, the development of molecular imaging probes is challenged by the high complexity of both molecular targets and probes, the limited accessibility of extravascular targets, unspecific sequestration of macromolecules used to deliver contrast agents like liposomes in the liver and spleen, and the relatively low number of cells suited as imaging targets within a diseased tissue.

For these reasons, alternative molecular imaging approaches are needed. One strategy to overcome the limitations of currently available contrast agents in clinical radiology and molecular imaging research is to develop ECM-specific contrast agents such as GagCEST as explained in Chap. 10. The ECM as a target for medical imaging is appealing for many reasons—three of which will be briefly discussed in the following paragraphs.

6.4.1 The Amount of ECM

The amount of ECM varies considerably between tissue types and pathophysiological states. In the *liver* (a cell-rich organ), the ECM volume fraction is less than 3% under normal conditions and can increase up to 30% in cirrhotic livers due to

excessive connective tissue accumulation. In *muscle,* the total amount of ECM is approximately 5% and has a very strong mechanical influence on muscle function (see Fig. 6.3). Therefore, pathological ECM accumulation in muscle is of high clinical relevance and directly alters its function [124]. Myocardial fibrosis is a major cause of cardiac dysfunction, leading to myocardial hypertrophy with systolic and diastolic dysfunction and infarction. In the *brain*, ECM constitutes about 10–20% of total brain volume [125] with substantial changes in quantity and structure during brain development [126]. Brain ECM undergoes constant reorganization in response to learning, neuronal activity, and plasticity. The elastic properties of each tissue depend on the mechanical characteristics of its cells and their surrounding ECM. The cellular responses to disease or physiological changes relate to small fractions of the total tissue mass, while the ECM responses to disease, such as abnormal ECM deposition in fibrosis, cancer, or atherosclerosis, can have devastating effects on tissues [127].

In the evolution of atherosclerosis, growth of plaques and ECM deposition in the wall of arteries are a major pathological hallmark of the disease and are often related to severe clinical complications, as previously described [6, 53, 128–131].

Overall, the changing amount of ECM in the progression of diseases could be translated into sensitive biomarkers. Moreover, the ECM is a tissue component that contributes to effective medium properties as explained in the next section.

6.4.2 Multiscale Physical Properties of the ECM

The size of cells usually defines the microscopic scale in imaging sciences which is the voxel size of the acquired image. Imaging signals are normally averaged within the voxel volume and therefore represent effective medium properties over all scales of tissue structures from the micro to the macro level. Details of tissue interactions on the microscopic level have to be enhanced by contrast agents or molecular imaging probes to be made visible by the macroscopic image contrast. Alternatively, biophysical imaging probes rely on multiscale networks in biological tissues which translate microstructural information from the cellular level into clinical image contrast [132, 133]. Proteins and polysaccharides of the ECM often form hierarchic and highly structured networks extending up to the macroscale size. The effect of large-scale networks on the global response of a tissue is well illustrated by adding a minor amount (less than 1 mass percent) of polysaccharides to water [133]. The established sugar chains cause a phase transition from liquid water into a solid gel by bridging long-range distances up to the percolation limit (i.e., bridging over the full sample size). It should be mentioned here that cellular networks such as the neuronal network or hierarchic vascular trees can upscale microscopic interactions in a similar way as ECM networks. This is exploited, e.g., by diffusion MRI based on restricted water mobility (see Chap. 17) or by MR elastography based on the mechanical integrity of neuronal tissue [108, 134, 135]. Also, collective cell behavior, such as jamming of tumor cells (see Chap. 5), induces macroscopic properties that reflect adhesion of cells at the microscopic level. However, in general, cellular

networks are embedded in a mesh of ECM components that dominate how the tissue is organized across multiple scales. The organization of skeletal muscle tissue by the collagen endomysial network is an example of the dominating structural properties of a minor fraction of tissue components and is shown for illustration in Fig. 6.4. Given that muscle tissue comprises only 5% ECM, the dominating collagen properties in mechanical muscle tests, especially under prestretched conditions, indicate that collagen is organized in extended and highly cross-linked networks, providing permanent support to the entire muscle (Figs. 6.3 and 6.4). Similarly, liver collagen infiltration in the course of fibrogenesis establishes a hierarchic network that turns liver tissue from a very soft and viscous material into a stiff and elastic

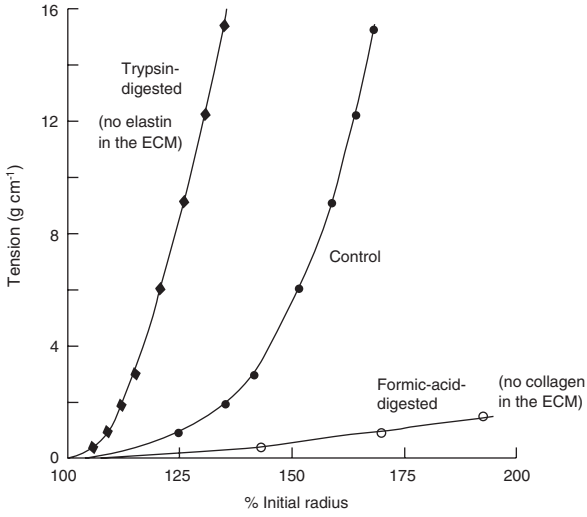

Fig. 6.3 Tension–length response of human iliac arteries with different amounts of collagen and elastin. When elastin is removed by trypsin digestion, the curve (diamonds) represents the properties of the remaining collagen. Alternatively, when collagen is removed by formic acid digestion, the curve (open circles) represents the properties of the elastin fibers. The broken curve (filled circles) is for an untreated artery (from [123] with permission)

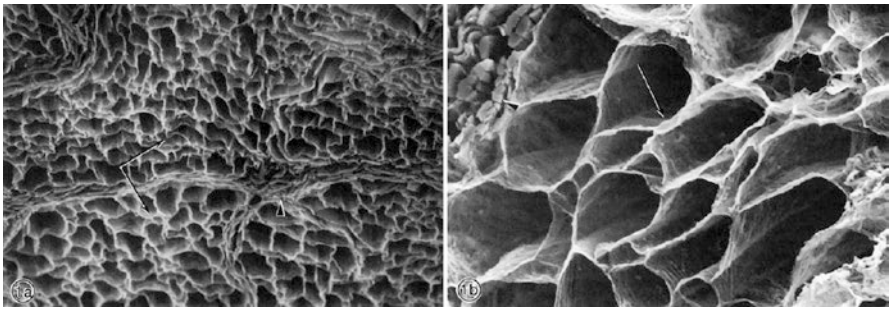

Fig. 6.4 Scanning electron microscopy of the collagen network around muscle fibers observed after digesting muscle fibers with NaOH. (**a**) Low magnification overview reveals an array of tubes into which muscle fibers insert (endomysium, arrows) as well as a thickened area surrounding the fibers (perimysium, arrowhead). (**b**) Higher-power view reveals the fine structure of the endomysial surfaces (arrow) as well as some undigested muscle fibers (arrowhead). This image demonstrates that muscle fibers are embedded in a tight matrix of connective tissue and are intimately associated with the ECM (from [136] with permission)

rubber-like solid [108, 137]. This change in global biophysical properties is the result not only of the increasing amount of collagen but also of the hierarchy of ECM architecture, which supports the entire organ on the macroscopic scale [104]. These observations raise the possibility of exploiting the multiscale nature of many ECM structures for translating microscopic biophysical and biochemical signals into macroscopic medical image contrast by using ECM-specific imaging probes.

6.4.3 ECM Function

The functions of the ECM can be divided into structural support and biochemical activity. Structural support is the mechanical function of the ECM and mainly relies on the structural ECM components such as collagen, elastin, and fibrillins. Under normal conditions, these components serve a scaffolding function, maintaining tissue architecture and homeostasis while providing tensile and compressive strength, thereby attenuating shear forces. The viscoelastic properties of mammalian tissues are tailored to their specific functions: pulmonary tissue, for example, is soft and elastic to enable large volume changes during breathing. Figure 6.3 demonstrates how the macroscopic behavior of muscle tissue changes with different amounts of collagen and elastin in the muscle ECM.

A hallmark of several diseases, including lung emphysema and arthritis or fibrosis and sclerosis, is a chronic change in the tissue's mechanical properties [127, 138]. During inflammatory processes, in particular, the activity of proteases can lead to a reduction in the content of elastin and thus to a decrease in the macroscopic shear modulus of the involved tissue. An increase in the amount of collagen has also been observed in the course of fibrosis and scar formation due to wound healing after tissue damage, regardless of the tissue or organ type.

An additional factor influencing the mechanical function of the ECM includes the balance between ECM-degrading and ECM synthesis processes. Therefore, it is not surprising that a distorted equilibrium in these processes is regarded as a hallmark of cancer [2]. ECM degradation can be induced enzymatically, for example, by matrix metalloproteases (MMP), while ECM deposition can be accomplished by crosslinking, as well as by the expression of ECM proteins and inhibitors of ECM-degrading enzymes. Furthermore, chemical signals such as cellular growth factors and cytokines are sequestered in the ECM and can later be released to diffuse through the tissue, supporting both cell and ECM homeostasis. This dynamic mechanical and biochemical interaction between cells and their ECM can influence gene transcription and therefore protein expression [139, 140]. This has implications for cell- and tissue-specific processes. For example, the ECM plays a role in promotion or inhibition of cell division [141], neuronal reorganization, and axonal outgrowth in the adult brain [142]. ECM-cell interactions are able to restrict neuronal reorganization and axonal outgrowth in the adult brain [142], making the ECM an essential determining factor of neural plasticity [126, 143, 144]. In case of disease, the ECM has been shown to contribute to cancer cell stiffness [60]. Cancer cells have been described to soften when exposed to rigid fibrotic stroma, thereby

transforming to a more aggressive state with higher metastatic potential [145]. These examples demonstrate the essential role of the ECM in normal tissue function and health preservation and stress the importance for development of ECM-specific imaging probes.

6.5 The State of the Art in Research on Molecular and Biophysical Imaging of the ECM

6.5.1 ECM Targeting with Imaging Probes

6.5.1.1 Collagen and Elastin

From a biochemical perspective, collagen and elastin are relatively well defined, which facilitates their detection by imaging probes. For the specific visualization of collagen components of the ECM, Caravan et al. [146] have developed a low-molecular-weight, gadolinium-based MR imaging probe, named EP-3533, which binds to type I collagen [147, 148]. In this probe, a Gd-containing complex is coupled to a peptide with high affinity to type I collagen and identified by phage display. This probe allowed assessment of the extent of fibrotic changes in the liver parenchyma in an animal model of liver fibrosis by determining the amount of collagen using noninvasive MRI [147, 148]. In an experimental model of myocardial infarction, the probe identified the area of infarction based on its collagen content [149]. An earlier in vitro approach proposed by Sanders et al. was based on MRI contrast agent containing liposomes linked to an adhesion protein for collagen [150]. Alternatively, the ECM protein elastin was targeted using a small-molecular, elastin-specific, gadolinium-based imaging probe developed for MRI and tested on various models. The suitability of this probe to analyze the elastin content of tissue by means of MRI has been demonstrated in an atherosclerosis model [151], a murine aneurysm model [152], and a myocardial infarction model [153, 154]. The results obtained in the atherosclerosis model provided strong evidence that the elastin-specific probe is suitable for noninvasive quantification of the clinically validated parameter plaque burden at different stages of plaque development [155, 156]. It has also been demonstrated that the elastin content of a plaque matrix can be noninvasively quantified by MRI, which has the potential to be used for differentiating between vulnerable and stable atherosclerotic plaques [157]. In a rabbit model of atherosclerosis, it was demonstrated that gadofluorin M accumulates in areas of atherosclerotic plaques with high amounts of ECM deposits [158]. Noteworthy, the accumulation of gadofluorin M was not associated with the lipid content of the vessel wall.

6.5.1.2 GAGs

In contrast to the ECM components collagen and elastin, GAGs are characterized by relatively high biochemical variability. Hence, GAG-specific peptides or antibodies for immunofluorescence in histological specimens are not yet available. However, already in the early 1980s, Ando et al. demonstrated that the characteristic

complex-forming properties of GAGs with regard to lanthanides can be exploited to label the pathological increase in GAG components in tumors by ^{67}Ga (a trivalent metal ion) or ^{69}Tm (a trivalent lanthanide), both administered in the form of citrate complexes [159, 160]. Using this approach, Ando et al. identified HS, KS, and heparin—particularly heavily sulfated GAGs—as the binding GAGs for ^{67}Ga [159, 160]. In this context, characterization of the pharmacokinetic properties of nonspecific Gd-based contrast agents as routinely applied in clinical MRI examinations remains a highly relevant research question. Since the advent of nonspecific Gd-based contrast agents in clinical routine, it has been known that a small amount of the gadolinium is not rapidly eliminated from the body, suggesting a two-compartment pharmacokinetic process. Early pharmacokinetic studies with ^{153}Gd-DTPA and Gd-[^{14}C] DTPA in healthy rats showed that, for a small amount (<1%) of the administered intravenous dose, free Gd^{3+} ions were released from the contrast medium complex (dechelation process) and partially accumulated in the bones, liver, and spleen of the animals [161]. Further pharmacokinetic studies with ^{153}Gd-DTPA in healthy rats by Wedeking et al. postulated a three-compartment model with slow exchange of the third compartment, characteristic of a drug-binding process [162]. Experimental and clinical pharmacokinetic studies using dynamic contrast-enhanced MRI with Gd-DTPA and similar substances also showed that, in various disease entities such as myocardial infarction, myocardial fibrosis and malignancy, the course of signal intensity fitted a three-compartment model better than a two-compartment model [163–168]. The third compartment is generally characterized by slow exchange constants. Current research shows that such a third compartment exists for both linear Gd contrast agents and, to a lesser extent, for macrocyclic Gd contrast agents [169]. The substrate of this third compartment is not yet known. However, it has been demonstrated that interaction of the Gd-based contrast agent with proteins does not play a role [162]. Studies conducted to determine the volume fractions of the different tissue components of the myocardium show a high binding level of La^{3+} to polyanionic sugar polymers, i.e., to the GAG components of the ECM [170], which in healthy myocardium account for 23% of the ECM volume [170]. After the discovery of nephrogenic systemic fibrosis (NSF), a severe illness observed after intravenous injection of linear Gd-based contrast agents in patients with end-stage renal disease, it was confirmed that Gd can leave the contrast agent complex by partial dechelation in vivo [171, 172]. The substrate that binds the free Gd^{3+} ions in a transchelation process has not yet been identified. However, GAGs are likely to play a role in the binding of free Gd^{3+}ions, thereby contributing to prolonged retention of these ions in tissue. Currently, the discovery of Gd deposition in brain tissue, particularly the nucleus dentatus and globus pallidus, after repeated administration of Gd-based contrast agents in patients with normal renal function gives rise to the question as to which tissue component binds the contrast agent molecule as a whole or as dechelated Gd [173, 174].

Some interesting evidence regarding GAG labeling can be derived from histochemical procedures used to identify these ECM components in histological specimens. For histochemical identification of GAGs, the sections are incubated with colloidal iron oxide and then stained with Perls' Prussian blue iron stain as a

secondary stain [175]. The staining of GAGs in histological sections with the cationic alcian blue stain is also based on their complex-forming properties [176]. Thus, pathologically altered GAGs can also be targeted in vivo by intravenous injection of appropriate iron oxide nanoparticles, which serve as contrast-enhancing agents for detection by MRI. Very small superparamagnetic iron oxide nanoparticles (VSOPs) with citrate as the coating material [177, 178] have the property to target GAGs and cells in vivo. In a rabbit atherosclerosis model, it was demonstrated that GAG-binding VSOPs can be used to detect pathologically elevated levels of GAGs and can discriminate between stable atherosclerotic plaques and those at risk of rupture [179]. In a mouse model of atherosclerosis, endothelial cells and macrophages of atherosclerotic plaques were identified as main target for VSOP by electron microscopy [180]. A subsequent study found that the VSOPs were endocytosed by endothelial cells already 10 min after intravenous injection [181]. In a mouse model of neuroinflammation, VSOPs also improved the capacity to detect an altered brain-blood barrier (BBB) [182] and the different localizations of VSOPs in brain with disrupted BBB suggested multiple entry mechanisms of VSOPs into the central nervous system [182, 183]. It was also shown for atherosclerosis and neuroinflammation, by using animal models, that adhesion of VSOPs to GAG-based molecules on the endothelial glycocalyx is a major factor in mediating their cellular uptake and transendothelial transport [181, 184]. These results were found for VSOP variants which do not carry any other target-specific molecules apart from their stabilizing coating. Current studies suggest that binding of VSOPs to GAGs takes place via transchelation [179], i.e., they lose their weakly bound citrate coating in the presence of GAGs upon the formation of a strong complex. The VSOP enrichment in different animal models shows the potential of these iron oxide nanoparticles for MRI and stimulates further studies to characterize their targets in vivo.

6.5.2 Biophysical Imaging of the ECM

For decades, dynamic mechanical tests collectively known as “rheometry” have been used for the mechanical-based analysis of micro-architectural properties of polymer samples [185]. More recently, mechanical test methods have been used for studies of biological soft matter or model networks prevalent in cells and tissues [186–188]. The rheological behavior of biological tissues is linked to the hierarchy of underlying structures [189]. Scale-invariant properties of rheological constants of cells or tissues can give insight into the organization of structure elements below the resolution limit of the measurement system [190, 191]. On the microscopic scale, rheological constants can be measured by various methods such as cell-deformation-based experiments [192, 193] or scanning force microscopy [187]. Macrorheological methods include oscillatory shear stress rheology [194], dynamic shear tests [195], stress-relaxation measurements [196], tensile tests [197], and macro-indentation [198]. Most rheological methods are surface based, i.e., mechanical stimulation is locally applied, and the resulting tissue response is measured at the surface. Elastography (see Chaps. 12 and 20) induces and measures shear waves inside the bulky tissue—in vivo for diagnostic applications [199] or ex vivo

for basic studies of soft tissue's rheological behavior [200]. In general, the measurement of intrinsic material properties inside a tissue volume by MRE is less susceptible to the geometry, texture, and composition of the sample surface [191]. In biological tissues, the relationship between stiffness and number of crosslinks can often be modeled by a powerlaw [132, 190]. MR elastography findings are consistent with observations made by oscillatory rheometry on macromolecular elastomers, which reveal that network elasticity originates from the cross-linked backbone of the network, while dissipativity originates from the unlinked parts of the network [201]. In general, motility of tissue elements results in enhanced lossy properties of the tissue. For example, water molecules demobilized by GAGs represent a gel-like tissue component with highly elastic and low viscous properties. For this reason, GAG-depleted tissue has higher lossy properties than tissue with high GAG content in the ECM [202]. The literature on tensile testing of tissues suggests that GAGs have a major influence on viscosity rather than on elasticity [203]. Figure 6.5 compares the MRE-measured viscoelastic dispersion function of collagen with that of HA, both with similar concentrations in water at room

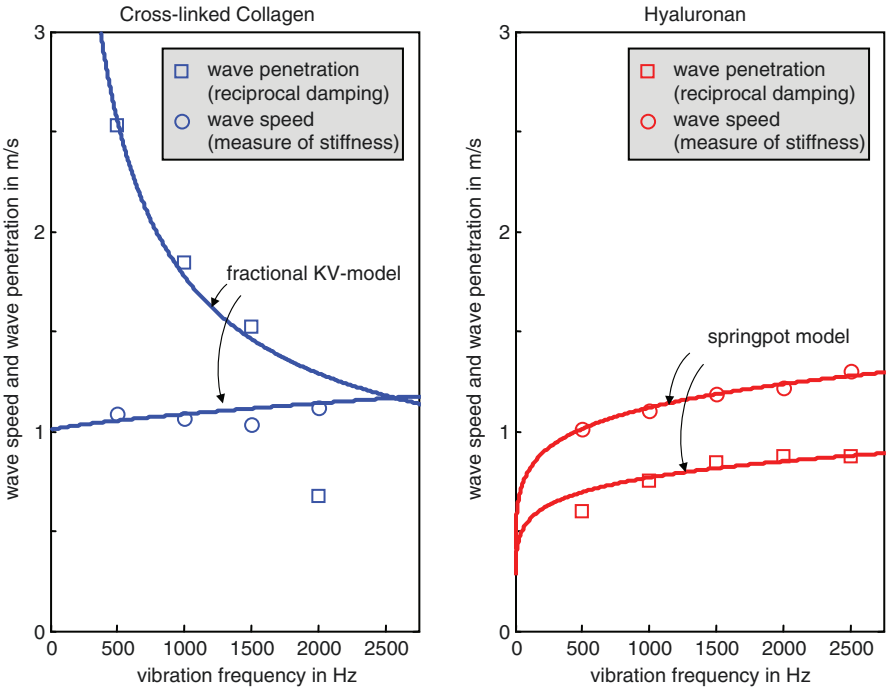

Fig. 6.5 Viscoelastic dispersion functions for single ECM components measured by tabletop MRE in small sample volumes [204]. Different viscoelastic properties of collagen and GAG are clearly seen by wave speed and wave penetration, which quantifies elasticity and reciprocal viscosity, respectively [205]. Overall, collagen properties are well predicted by a solid body model, in particular at lower frequencies, as described by the three-parameter fractional Kelvin-Voigt (KV) model [206]. In contrast, HA displays viscoelastic scaling properties as predicted by the two-parameter springpot model. Note that wave speed values in both materials are similar despite their distinct viscous behaviors

temperature. Comparison between 4% porcine collagen and HA hydrogels (Fig. 6.5) demonstrates that shear wave speed related to elasticity is similar in both materials, while wave penetration, which is reciprocally related to viscosity (inverse damping), differs markedly between collagen and HA. The fractional Kelvin-Voigt model predicts a decrease in viscosity with lowering the driving frequency, whereas in the springpot, both elasticity and viscosity have a constant ratio over all frequencies (see Chap. 2, Fig. 2.5, and Eq. (2.44) therein). This example demonstrates the importance of measuring both elasticity and viscosity to characterize the composition of the ECM in terms of networks made up of both fibrous proteins such as collagen and water-binding GAGs. So far, only indirect correlation analyses between ECM structures and tissue viscoelasticity have been performed. In Reiter et al. [104], the amount of connective tissue in fibrotic livers was quantified and compared with springpot-based wideband MRE, showing that the amount of collagen is less correlated with the degree of fibrosis than MRE.

Conclusion

The ECM of biological soft tissues consists of structural components which determine the macroscopic biophysical properties of the tissue such as elasticity in the linear and nonlinear regime. Disease can significantly alter the content of these components, leading to marked changes in mechanical tissue properties. Furthermore, GAGs, which fill most of the extracellular space due to strong water-binding capacity, provide mechanical support against compression and influence the lossy properties of the tissue as quantified by viscosity. GAGs and other ECM components might change quantitatively and qualitatively in many disease processes such as inflammation, affecting both the biomechanical and the biochemical properties of the ECM. Innovative imaging probes may thus target GAG components of the ECM in both the interstitial space and the basement membrane.

References

1. Ascoli M. Bulletin of the National Research Council, 69, Bulletin of the National Research Council, National Research Council, U.S. Washington: National Academies; 1929.
2. Frantz C, Stewart KM, Weaver VM. The extracellular matrix at a glance. J Cell Sci. 2010;123(Pt 24):4195–200.
3. Alberts B, et al. Molecular biology of the cell. 4th ed. New York: Garland Science; 2002.
4. Murphy W, Black J, Hastings G. Handbook of biomaterial properties. 2nd ed. New York: Springer; 2016.
5. Spinale FG, Zile MR. Integrating the myocardial matrix into heart failure recognition and management. Circ Res. 2013;113(6):725–38.
6. Katsuda S, Kaji T. Atherosclerosis and extracellular matrix. J Atheroscler Thromb. 2003;10(5):267–74.
7. Smith PD, et al. "GAG-ing with the neuron": the role of glycosaminoglycan patterning in the central nervous system. Exp Neurol. 2015;274(Pt B):100–14.
8. Baiocchini A, et al. Extracellular matrix molecular remodeling in human liver fibrosis evolution. PLoS One. 2016;11(3):e0151736.

9. Kalluri R. Basement membranes: structure, assembly and role in tumour angiogenesis. Nat Rev Cancer. 2003;3(6):422–33.
10. Pozzi A, Yurchenco PD, Iozzo RV. The nature and biology of basement membranes. Matrix Biol. 2017;57-58:1–11.
11. Paulsson M. Basement membrane proteins: structure, assembly, and cellular interactions. Crit Rev Biochem Mol Biol. 1992;27(1-2):93–127.
12. Timpl R, Brown JC. The laminins. Matrix Biol. 1994;14(4):275–81.
13. Timpl R. Macromolecular organization of basement membranes. Curr Opin Cell Biol. 1996;8(5):618–24.
14. Timpl R, et al. Laminin, proteoglycan, nidogen and collagen IV: structural models and molecular interactions. Ciba Found Symp. 1984;108:25–43.
15. Aumailley M, et al. Binding of nidogen and the laminin-nidogen complex to basement membrane collagen type IV. Eur J Biochem. 1989;184(1):241–8.
16. Tsiper MV, Yurchenco PD. Laminin assembles into separate basement membrane and fibrillar matrices in Schwann cells. J Cell Sci. 2002;115(Pt 5):1005–15.
17. Charonis AS, et al. Binding of laminin to type IV collagen: a morphological study. J Cell Biol. 1985;100(6):1848–53.
18. Sasaki T, et al. Deficiency of β1 integrins in teratoma interferes with basement membrane assembly and laminin-1 expression. Exp Cell Res. 1998;238(1):70–81.
19. Aumailley M, et al. A simplified laminin nomenclature. Matrix Biol. 2005;24(5):326–32.
20. Veitch DP, et al. Mammalian tolloid metalloproteinase, and not matrix metalloprotease 2 or membrane type 1 metalloprotease, processes laminin-5 in keratinocytes and skin. J Biol Chem. 2003;278(18):15661–8.
21. Koshikawa N, et al. Membrane-type matrix metalloproteinase-1 (MT1-MMP) is a processing enzyme for human laminin gamma 2 chain. J Biol Chem. 2005;280(1):88–93.
22. Koshikawa N, et al. Proteolytic processing of laminin-5 by MT1-MMP in tissues and its effects on epithelial cell morphology. FASEB J. 2004;18(2):364–6.
23. Qin Y, et al. Laminins and cancer stem cells: partners in crime? Semin Cancer Biol. 2016;45:3.
24. Feller W. An introduction to probability theory and its applications. New York: Willey; 1968.
25. Hynes RO. Integrins: bidirectional, allosteric signaling machines. Cell. 2002;110(6):673–87.
26. Voet D, Voet J, Pratt CW. Fundamentals of biochemistry. New York: Wiley; 1999.
27. Lieleg O, Ribbeck K. Biological hydrogels as selective diffusion barriers. Trends Cell Biol. 2011;21(9):543–51.
28. Esko JD, Kimata K, Lindahl U. Proteoglycans and sulfated glycosaminoglycans. In: Varki A, et al., editors. Essentials of glycobiology. New York: Cold Spring Harbor; 2009.
29. Sasaki N, et al. Cell surface localization of heparanase on macrophages regulates degradation of extracellular matrix heparan sulfate. J Immunol. 2004;172(6):3830–5.
30. Hacker U, Nybakken K, Perrimon N. Heparan sulphate proteoglycans: the sweet side of development. Nat Rev Mol Cell Biol. 2005;6(7):530–41.
31. Bishop JR, Schuksz M, Esko JD. Heparan sulphate proteoglycans fine-tune mammalian physiology. Nature. 2007;446(7139):1030–7.
32. Gubbiotti MA, Neill T, Iozzo RV. A current view of perlecan in physiology and pathology: a mosaic of functions. Matrix Biol. 2017;57-58:285–98.
33. Ricard-Blum S, Lisacek F. Glycosaminoglycanomics: where we are. Glycoconj J. 2017;34:339–49.
34. Iozzo RV, Schaefer L. Proteoglycan form and function: a comprehensive nomenclature of proteoglycans. Matrix Biol. 2015;42:11–55.
35. Bishnoi M, et al. Chondroitin sulphate: a focus on osteoarthritis. Glycoconj J. 2016;33(5):693–705.
36. Zamfir AD, et al. Brain chondroitin/dermatan sulfate, from cerebral tissue to fine structure: extraction, preparation, and fully automated chip-electrospray mass spectrometric analysis. In: Rédini F, editor. Proteoglycans: methods and protocols. Totowa: Humana Press; 2012. p. 145–59.

37. Malmström A, et al. Iduronic acid in chondroitin/dermatan sulfate: biosynthesis and biological function. J Histochem Cytochem. 2012;60(12):916–25.
38. Mongiat M, et al. Extracellular matrix, a hard player in angiogenesis. Int J Mol Sci. 2016;17(11):E1822.
39. Mercier F. Fractones: extracellular matrix niche controlling stem cell fate and growth factor activity in the brain in health and disease. Cell Mol Life Sci. 2016;73(24):4661–74.
40. Sethi MK, Zaia J. Extracellular matrix proteomics in schizophrenia and Alzheimer's disease. Anal Bioanal Chem. 2017;409(2):379–94.
41. Xu D, Esko JD. Demystifying heparan sulfate-protein interactions. Annu Rev Biochem. 2014;83:129–57.
42. Mizumoto S, Yamada S, Sugahara K. Molecular interactions between chondroitin-dermatan sulfate and growth factors/receptors/matrix proteins. Curr Opin Struct Biol. 2015;34:35–42.
43. Meneghetti MC, et al. Heparan sulfate and heparin interactions with proteins. J R Soc Interface. 2015;12(110):0589.
44. Parish CR. The role of heparan sulphate in inflammation. Nat Rev Immunol. 2006;6(9):633–43.
45. Pomin VH. Sulfated glycans in inflammation. Eur J Med Chem. 2015;92:353–69.
46. Jin-Ping L. Heparin, heparan sulfate and heparanase in cancer: remedy for metastasis? Anti Cancer Agents Med Chem. 2008;8(1):64–76.
47. Maytin EV. Hyaluronan: more than just a wrinkle filler. Glycobiology. 2016;26(6):553–9.
48. Laurent TC. The chemistry, biology and medical applications of hyaluronan and its derivatives. London: Portland Press; 1998.
49. Balazs EA, Denlinger JL. Viscosupplementation: a new concept in the treatment of osteoarthritis. J Rheumatol Suppl. 1993;39:3–9.
50. Brandt KD, Smith GN Jr, Simon LS. Intraarticular injection of hyaluronan as treatment for knee osteoarthritis: what is the evidence? Arthritis Rheum. 2000;43(6):1192–203.
51. Cohen MD. Hyaluronic acid treatment (viscosupplementation) for OA of the knee. Bull Rheum Dis. 1998;47(7):4–7.
52. George E. Intra-articular hyaluronan treatment for osteoarthritis. Ann Rheum Dis. 1998;57(11):637–40.
53. Viola M, et al. Extracellular matrix in atherosclerosis: hyaluronan and proteoglycans insights. Curr Med Chem. 2016;23(26):2958–71.
54. Ando A, et al. Mechanism of tumor and liver concentration of 111In and 169Yb: 111In and 169Yb binding substances in tumor tissues and liver. Eur J Nucl Med. 1982;7(7):298–303.
55. Taylor KR, Gallo RL. Glycosaminoglycans and their proteoglycans: host-associated molecular patterns for initiation and modulation of inflammation. FASEB J. 2006;20(1):9–22.
56. Varki A, Freeze HH. Glycans in acquired human diseases. In: Varki A, Cummings RD, Esko JD, et al., editors. Essentials of glycobiology. Cold Spring Harbor: Cold Spring Harbor Laboratory Press; 2009.
57. Mitra AK, et al. Dermatan sulfate: molecular conformations and interactions in the condensed state. J Mol Biol. 1983;169(4):873–901.
58. Corte MD, et al. Analysis of the expression of hyaluronan in intraductal and invasive carcinomas of the breast. J Cancer Res Clin Oncol. 2010;136(5):745–50.
59. Takeuchi J, et al. Variation in glycosaminoglycan components of breast tumors. Cancer Res. 1976;36(7 PT 1):2133–9.
60. Pickup MW, Mouw JK, Weaver VM. The extracellular matrix modulates the hallmarks of cancer. EMBO Rep. 2014;15(12):1243–53.
61. Rowlands D, Sugahara K, Kwok J. Glycosaminoglycans and glycomimetics in the central nervous system. Molecules. 2015;20(3):3527.
62. Moretto P, et al. Regulation of hyaluronan synthesis in vascular diseases and diabetes. J Diabetes Res. 2015;2015:167283.
63. Abdel-Hamid NM. Premalignant variations in extracellular matrix composition in chemically induced hepatocellular carcinoma in rats. J Membr Biol. 2009;230(3):155–62.
64. Schwertfeger KL, et al. Hyaluronan, inflammation, and breast cancer progression. Front Immunol. 2015;6:236.

65. Kolarova H, et al. Modulation of endothelial glycocalyx structure under inflammatory conditions. Mediat Inflamm. 2014;2014:694312.
66. Gouverneur M, et al. Fluid shear stress stimulates incorporation of hyaluronan into endothelial cell glycocalyx. Am J Physiol Heart Circ Physiol. 2006;290(1):H458–2.
67. Elhadj S, Akers RM, Forsten-Williams K. Chronic pulsatile shear stress alters insulin-like growth factor-I (IGF-I) binding protein release in vitro. Ann Biomed Eng. 2003;31(2):163–70.
68. Pahakis MY, et al. The role of endothelial glycocalyx components in mechanotransduction of fluid shear stress. Biochem Biophys Res Commun. 2007;355(1):228–33.
69. Tarbell JM, Cancel LM. The glycocalyx and its significance in human medicine. J Intern Med. 2016;280(1):97–113.
70. Rabenstein DL, Robert JM, Peng J. Multinuclear magnetic resonance studies of the interaction of inorganic cations with heparin. Carbohydr Res. 1995;278(2):239–56.
71. Casu B, et al. Stereoselective effects of gadolinium ions on the relaxation properties of 13C and 1H nuclei of aldohexuronic acids and poly(glycosiduronic acids). Carbohydr Res. 1975;41(1):C6–8.
72. Rej RN, Holme KR, Perlin AS. Marked stereoselectivity in the binding of copper ions by heparin. Contrasts with the binding of gadolinium and calcium ions. Carbohydr Res. 1990;207(2):143–52.
73. Joffe P, Thomsen HS, Meusel M. Pharmacokinetics of gadodiamide injection in patients with severe renal insufficiency and patients undergoing hemodialysis or continuous ambulatory peritoneal dialysis. Acad Radiol. 1998;5(7):491–502.
74. Gibby WA, Gibby KA, Gibby WA. Comparison of Gd DTPA-BMA (Omniscan) versus Gd HP-DO3A (ProHance) retention in human bone tissue by inductively coupled plasma atomic emission spectroscopy. Investig Radiol. 2004;39(3):138–42.
75. Marckmann P, et al. Nephrogenic systemic fibrosis: suspected causative role of gadodiamide used for contrast-enhanced magnetic resonance imaging. J Am Soc Nephrol. 2006;17(9):2359–62.
76. McDonald RJ, et al. Intracranial gadolinium deposition after contrast-enhanced MR imaging. Radiology. 2015;275(3):772–82.
77. Radbruch A, et al. Gadolinium retention in the dentate nucleus and globus pallidus is dependent on the class of contrast agent. Radiology. 2015;275(3):783–91.
78. Kanda T, et al. Gadolinium-based contrast agent accumulates in the brain even in subjects without severe renal dysfunction: evaluation of autopsy brain specimens with inductively coupled plasma mass spectroscopy. Radiology. 2015;276(1):228–32.
79. Runge VM. Safety of the gadolinium-based contrast agents for magnetic resonance imaging, focusing in part on their accumulation in the brain and especially the dentate nucleus. Investig Radiol. 2016;51(5):273–9.
80. Taupitz M, et al. Gadolinium-containing magnetic resonance contrast media: investigation on the possible transchelation of Gd(3)(+) to the glycosaminoglycan heparin. Contrast Media Mol Imaging. 2013;8(2):108–16.
81. Schlemm L, et al. Gadopentetate but not gadobutrol accumulates in the dentate nucleus of multiple sclerosis patients. Mult Scler. 2017;23:963.
82. Theocharis AD, et al. Extracellular matrix structure. Adv Drug Deliv Rev. 2016;97:4–27.
83. Kolodgie FD, et al. Differential accumulation of proteoglycans and hyaluronan in culprit lesions: insights into plaque erosion. Arterioscler Thromb Vasc Biol. 2002;22(10):1642–8.
84. Wight TN, Merrilees MJ. Proteoglycans in atherosclerosis and restenosis: key roles for versican. Circ Res. 2004;94(9):1158–67.
85. Chen W, et al. Collagen-specific peptide conjugated HDL nanoparticles as MRI contrast agent to evaluate compositional changes in atherosclerotic plaque regression. JACC Cardiovasc Imaging. 2013;6(3):373–84.
86. Stary HC, et al. A definition of advanced types of atherosclerotic lesions and a histological classification of atherosclerosis. A report from the Committee on Vascular Lesions of the Council on Arteriosclerosis, American Heart Association. Circulation. 1995;92(5):1355–74.

87. Virmani R, et al. Lessons from sudden coronary death: a comprehensive morphological classification scheme for atherosclerotic lesions. Arterioscler Thromb Vasc Biol. 2000;20(5):1262–75.
88. Daugherty A, Cassis LA. Mechanisms of abdominal aortic aneurysm formation. Curr Atheroscler Rep. 2002;4(3):222–7.
89. Humphrey JD. Possible mechanical roles of glycosaminoglycans in thoracic aortic dissection and associations with dysregulated transforming growth factor-beta. J Vasc Res. 2013;50(1):1–10.
90. Rienks M, et al. Myocardial extracellular matrix. An ever-changing and diverse entity. Circ Res. 2014;114(5):872–88.
91. Shetlar MR, Shetlar CL, Kischer CW. Healing of myocardial infarction in animal models. Tex Rep Biol Med. 1979;39:339–55.
92. Judd JT, et al. Myocardial connective tissue metabolism in response to injury. II. Investigation of the mucopolysaccharides involved in isoproterenol-induced necrosis and repair in rat hearts. Circ Res. 1970;26(1):101–9.
93. Judd JT, Wexler BC. Sulfur 35 uptake in acid mucopolysaccharides of the rat heart following injury. Am J Phys. 1973;224(2):312–7.
94. Sykova E, et al. Learning deficits in aged rats related to decrease in extracellular volume and loss of diffusion anisotropy in hippocampus. Hippocampus. 2002;12(2):269–79.
95. Sack I, et al. The impact of aging and gender on brain viscoelasticity. NeuroImage. 2009;46(3):652–7.
96. van Horssen J, et al. Basement membrane proteins in multiple sclerosis-associated inflammatory cuffs: potential role in influx and transport of leukocytes. J Neuropathol Exp Neurol. 2005;64(8):722–9.
97. van Horssen J, et al. Extensive extracellular matrix depositions in active multiple sclerosis lesions. Neurobiol Dis. 2006;24(3):484–91.
98. Back SA, et al. Hyaluronan accumulates in demyelinated lesions and inhibits oligodendrocyte progenitor maturation. Nat Med. 2005;11(9):966–72.
99. Baumgart DC, et al. US-based real-time elastography for the detection of fibrotic gut tissue in patients with stricturing Crohn disease. Radiology. 2015;275(3):889–99.
100. Burke JP, et al. Fibrogenesis in Crohn's disease. Am J Gastroenterol. 2007;102(2):439–48.
101. Latella G, et al. Mechanisms of initiation and progression of intestinal fibrosis in IBD. Scand J Gastroenterol. 2015;50(1):53–65.
102. Iredale JP. Models of liver fibrosis: exploring the dynamic nature of inflammation and repair in a solid organ. J Clin Investig. 2007;117(3):539–48.
103. Mallat A, Lotersztajn S. Cellular mechanisms of tissue fibrosis. 5. Novel insights into liver fibrosis. Am J Physiol Cell Physiol. 2013;305(8):C789–99.
104. Reiter R, et al. Wideband MRE and static mechanical indentation of human liver specimen: sensitivity of viscoelastic constants to the alteration of tissue structure in hepatic fibrosis. J Biomech. 2014;47(7):1665–74.
105. Guedes PLR, et al. Increase of glycosaminoglycans and metalloproteinases 2 and 9 in liver extracellular matrix on early stages of extrahepatic cholestasis. Arq Gastroenterol. 2014;51:309–15.
106. Scott JE, et al. The chemical morphology of extracellular matrix in experimental rat liver fibrosis resembles that of normal developing connective tissue. Virchows Arch. 1994;424(1):89–98.
107. Bonekamp S, et al. Can imaging modalities diagnose and stage hepatic fibrosis and cirrhosis accurately? J Hepatol. 2009;50(1):17–35.
108. Sack I, et al. Structure sensitive elastography: on the viscoelastic powerlaw behavior of in vivo human tissue in health and disease. Soft Matter. 2013;9(24):5672–80.
109. Weissleder R, Mahmood U. Molecular imaging. Radiology. 2001;219(2):316–33.
110. Geven EJW, et al. S100A8/A9, a potent serum and molecular imaging biomarker for synovial inflammation and joint destruction in seronegative experimental arthritis. Arthritis Res Ther. 2016;18(1):247.

111. Withana NP, et al. Dual-modality activity-based probes as molecular imaging agents for vascular inflammation. J Nucl Med. 2016;57(10):1583–90.
112. Jorgensen NP, et al. Cholinergic PET imaging in infections and inflammation using 11C-donepezil and 18F-FEOBV. Eur J Nucl Med Mol Imaging. 2017;44(3):449–58.
113. Bwatanglang IB, et al. Folic acid targeted Mn:ZnS quantum dots for theranostic applications of cancer cell imaging and therapy. Int J Nanomedicine. 2016;11:413–28.
114. Chatterjee S, et al. A humanized antibody for imaging immune checkpoint ligand PD-L1 expression in tumors. Oncotarget. 2016;7(9):10215–27.
115. Chen C, et al. Molecular imaging with MRI: potential application in pancreatic cancer. Biomed Res Int. 2015;2015:10.
116. Eisenmenger LB, et al. Advances in PET imaging of degenerative, cerebrovascular, and traumatic causes of dementia. Semin Nucl Med. 2016;46(1):57–87.
117. Gomperts SN, et al. Tau positron emission tomographic imaging in the Lewy body diseases. JAMA Neurol. 2016;73(11):1334–41.
118. Farrar CT, et al. RNA aptamer probes as optical imaging agents for the detection of amyloid plaques. PLoS One. 2014;9(2):e89901.
119. Huppertz A, et al. Improved detection of focal liver lesions at MR imaging: multicenter comparison of gadoxetic acid-enhanced MR images with intraoperative findings. Radiology. 2004;230(1):266–75.
120. Hamm B, et al. Phase I clinical evaluation of Gd-EOB-DTPA as a hepatobiliary MR contrast agent: safety, pharmacokinetics, and MR imaging. Radiology. 1995;195(3):785–92.
121. Hamm B, et al. Contrast-enhanced MR imaging of liver and spleen: first experience in humans with a new superparamagnetic iron oxide. J Magn Reson Imaging. 1994;4(5):659–68.
122. Reimer P, Balzer T. Ferucarbotran (Resovist): a new clinically approved RES-specific contrast agent for contrast-enhanced MRI of the liver: properties, clinical development, and applications. Eur Radiol. 2003;13(6):1266–76.
123. Roach MR, Burton AC. The reason for the shape of the distensibility curves of arteries. Can J Biochem Physiol. 1957;35(8):681–90.
124. Gillies AR, Lieber RL. Structure and function of the skeletal muscle extracellular matrix. Muscle Nerve. 2011;44(3):318–31.
125. Hrabětová S, Nicholson C. Biophysical properties of brain extracellular space explored with ion-selective microelectrodes, integrative optical imaging and related techniques. In: Michael A, Borland L, editors. Electrochemical methods for neuroscience. Boca Raton: CRC Press/ Taylor & Francis; 2007.
126. Carulli D, et al. Chondroitin sulfate proteoglycans in neural development and regeneration. Curr Opin Neurobiol. 2005;15(1):116–20.
127. Butcher DT, Alliston T, Weaver VM. A tense situation: forcing tumour progression. Nat Rev Cancer. 2009;9(2):108–22.
128. Asplund A, et al. Macrophages exposed to hypoxia secrete proteoglycans for which LDL has higher affinity. Atherosclerosis. 2011;215(1):77–81.
129. Karangelis DE, et al. Glycosaminoglycans as key molecules in atherosclerosis: the role of versican and hyaluronan. Curr Med Chem. 2010;17(33):4018–26.
130. Tran-Lundmark K, et al. Heparan sulfate in perlecan promotes mouse atherosclerosis: roles in lipid permeability, lipid retention, and smooth muscle cell proliferation. Circ Res. 2008;103(1):43–52.
131. Theocharis AD, et al. Chondroitin sulfate as a key molecule in the development of atherosclerosis and cancer progression. Adv Pharmacol. 2006;53:281–95.
132. Posnansky O, et al. Fractal network dimension and viscoelastic powerlaw behavior: I. A modeling approach based on a coarse-graining procedure combined with shear oscillatory rheometry. Phys Med Biol. 2012;57(12):4023–40.
133. Guo J, et al. Fractal network dimension and viscoelastic powerlaw behavior: II. An experimental study of structure-mimicking phantoms by magnetic resonance elastography. Phys Med Biol. 2012;57(12):4041–53.

134. Freimann FB, et al. MR elastography in a murine stroke model reveals correlation of macroscopic viscoelastic properties of the brain with neuronal density. NMR Biomed. 2013;26(11):1534–9.
135. Klein C, et al. Enhanced adult neurogenesis increases brain stiffness: in vivo magnetic resonance elastography in a mouse model of dopamine depletion. PLoS One. 2014;9(3):e92582.
136. Trotter JA, Purslow PP. Functional morphology of the endomysium in series fibered muscles. J Morphol. 1992;212(2):109–22.
137. Asbach P, et al. Viscoelasticity-based staging of hepatic fibrosis with multifrequency MR elastography. Radiology. 2010;257(1):80–6.
138. Ingber DE. Mechanobiology and diseases of mechanotransduction. Ann Med. 2003;35(8):564–77.
139. DuFort CC, Paszek MJ, Weaver VM. Balancing forces: architectural control of mechanotransduction. Nat Rev Mol Cell Biol. 2011;12(5):308–19.
140. Nelson CM, Bissell MJ. Modeling dynamic reciprocity: engineering three-dimensional culture models of breast architecture, function, and neoplastic transformation. Semin Cancer Biol. 2005;15(5):342–52.
141. Mizuguchi S, et al. Chondroitin proteoglycans are involved in cell division of Caenorhabditis elegans. Nature. 2003;423(6938):443–8.
142. Soleman S, et al. Targeting the neural extracellular matrix in neurological disorders. Neuroscience. 2013;253:194–213.
143. Happel M, Frischknecht R. Neuronal plasticity in the juvenile and adult brain regulated by the extracellular matrix. In: Travascio F, editor. Composition and function of the extracellular matrix in the human body. Rijeka: Intech; 2016.
144. Pizzorusso T, et al. Reactivation of ocular dominance plasticity in the adult visual cortex. Science. 2002;298(5596):1248–51.
145. Levental KR, et al. Matrix crosslinking forces tumor progression by enhancing integrin signaling. Cell. 2009;139(5):891–906.
146. Caravan P, et al. Collagen-targeted MRI contrast agent for molecular imaging of fibrosis. Angew Chem Int Ed Engl. 2007;46(43):8171–3.
147. Fuchs BC, et al. Molecular MRI of collagen to diagnose and stage liver fibrosis. J Hepatol. 2013;59(5):992–8.
148. Polasek M, et al. Molecular MR imaging of liver fibrosis: a feasibility study using rat and mouse models. J Hepatol. 2012;57(3):549–55.
149. Spuentrup E, et al. Molecular magnetic resonance imaging of myocardial perfusion with EP-3600, a collagen-specific contrast agent: initial feasibility study in a swine model. Circulation. 2009;119(13):1768–75.
150. Sanders HM, et al. Morphology, binding behavior and MR-properties of paramagnetic collagen-binding liposomes. Contrast Media Mol Imaging. 2009;4(2):81–8.
151. Phinikaridou A, et al. Vascular remodeling and plaque vulnerability in a rabbit model of atherosclerosis: comparison of delayed-enhancement MR imaging with an elastin-specific contrast agent and unenhanced black-blood MR imaging. Radiology. 2014;271(2):390–9.
152. Okamura H, et al. Assessment of elastin deficit in a Marfan mouse aneurysm model using an elastin-specific magnetic resonance imaging contrast agent. Circ Cardiovasc Imaging. 2014;7(4):690–6.
153. Protti A, et al. Assessment of myocardial remodeling using an elastin/tropoelastin specific agent with high field magnetic resonance imaging (MRI). J Am Heart Assoc. 2015;4(8):e001851.
154. Wildgruber M, et al. Assessment of myocardial infarction and postinfarction scar remodeling with an elastin-specific magnetic resonance agent. Circ Cardiovasc Imaging. 2014;7(2):321–9.
155. Makowski MR, et al. Noninvasive assessment of atherosclerotic plaque progression in ApoE-/- mice using susceptibility gradient mapping. Circ Cardiovasc Imaging. 2011;4(3):295–303.
156. Stone GW, et al. A prospective natural-history study of coronary atherosclerosis. N Engl J Med. 2011;364(3):226–35.

157. Makowski MR, et al. Assessment of atherosclerotic plaque burden with an elastin-specific magnetic resonance contrast agent. Nat Med. 2011;17(3):383–8.
158. Meding J, et al. Magnetic resonance imaging of atherosclerosis by targeting extracellular matrix deposition with Gadofluorine M. Contrast Media Mol Imaging. 2007;2(3):120–9.
159. Ando A, et al. Mechanism of tumor and liver concentration of 67Ga: 67Ga binding substances in tumor tissues and liver. Int J Nucl Med Biol. 1983;10(1):1–9.
160. Ando A, et al. Affinity of 167Tm-citrate for tumor and liver tissue. Eur J Nucl Med. 1983;8(10):440–6.
161. Kasokat T, Urich K. Quantification of dechelation of gadopentetate dimeglumine in rats. Arzneimittelforschung. 1992;42(6):869–76.
162. Wedeking P, et al. Pharmacokinetic analysis of blood distribution of intravenously administered 153Gd-labeled Gd(DTPA)2- and 99mTc(DTPA) in rats. Magn Reson Imaging. 1990;8(5):567–75.
163. Knowles BR, et al. Pharmacokinetic modeling of delayed gadolinium enhancement in the myocardium. Magn Reson Med. 2008;60(6):1524–30.
164. Goldfarb JW, Zhao W, Han J. Three-compartment (3C) pharmacokinetic modeling is more accurate than two-compartment (2C) modeling of myocardial fibrosis gadolinium kinetics. J Cardiovasc Magn Reson. 2012;14(1):P248.
165. Port RE, et al. Multicompartment analysis of gadolinium chelate kinetics: blood-tissue exchange in mammary tumors as monitored by dynamic MR imaging. J Magn Reson Imaging. 1999;10(3):233–41.
166. Port RE, et al. Noncompartmental kinetic analysis of DCE-MRI data from malignant tumors: application to glioblastoma treated with bevacizumab. Magn Reson Med. 2010;64(2):408–17.
167. Franiel T, et al. Differentiation of prostate cancer from normal prostate tissue: role of hotspots in pharmacokinetic MRI and histologic evaluation. AJR Am J Roentgenol. 2010;194(3):675–81.
168. Lüdemann L, et al. Comparison of dynamic contrast-enhanced MRI with WHO tumor grading for gliomas. Eur Radiol. 2001;11(7):1231–41.
169. Lancelot E. Revisiting the pharmacokinetic profiles of gadolinium-based contrast agents: differences in long-term biodistribution and excretion. Investig Radiol. 2016;51(11):691–700.
170. Frank JS, Langer GA. The myocardial interstitium: its structure and its role in ionic exchange. J Cell Biol. 1974;60(3):586–601.
171. Robic C, et al. The role of phosphate on Omniscan(®) dechelation: an in vitro relaxivity study at pH 7. Biometals. 2011;24(4):759–68.
172. Idee JM, et al. Involvement of gadolinium chelates in the mechanism of nephrogenic systemic fibrosis: an update. Radiol Clin N Am. 2009;47(5):855–69. vii
173. Murata N, et al. Macrocyclic and other non-group 1 gadolinium contrast agents deposit low levels of gadolinium in brain and bone tissue: preliminary results from 9 patients with normal renal function. Investig Radiol. 2016;51(7):447–53.
174. Kanda T, et al. High signal intensity in dentate nucleus on unenhanced T1-weighted MR images: association with linear versus macrocyclic gadolinium chelate administration. Radiology. 2015;275(3):803–9.
175. Hale CW. Histochemical demonstration of acid polysaccharides in animal tissues. Nature. 1946;157:802.
176. Scott JE, Dorling J. Differential staining of acid glycosaminoglycans (mucopolysaccharides) by alcian blue in salt solutions. Histochemie. 1965;5(3):221–33.
177. Taupitz M, et al. New generation of monomer-stabilized very small superparamagnetic iron oxide particles (VSOP) as contrast medium for MR angiography: preclinical results in rats and rabbits. J Magn Reson Imaging. 2000;12(6):905–11.
178. Wagner S, et al. Monomer-coated very small superparamagnetic iron oxide particles as contrast medium for magnetic resonance imaging: preclinical in vivo characterization. Investig Radiol. 2002;37(4):167–77.

179. Wagner S, et al. Contrast-enhanced MR imaging of atherosclerosis using citrate-coated superparamagnetic iron oxide nanoparticles: calcifying microvesicles as imaging target for plaque characterization. Int J Nanomedicine. 2013;8:767–79.
180. Scharlach C, et al. Synthesis of acid-stabilized iron oxide nanoparticles and comparison for targeting atherosclerotic plaques: evaluation by MRI, quantitative MPS, and TEM alternative to ambiguous Prussian blue iron staining. Nanomedicine. 2015;11(5):1085–95.
181. Poller WC, et al. Uptake of citrate-coated iron oxide nanoparticles into atherosclerotic lesions in mice occurs via accelerated transcytosis through plaque endothelial cells. Nano Res. 2016;9(11):3437–52.
182. Tysiak E, et al. Beyond blood brain barrier breakdown - in vivo detection of occult neuroinflammatory foci by magnetic nanoparticles in high field MRI. J Neuroinflammation. 2009;6:20.
183. Millward JM, et al. Iron oxide magnetic nanoparticles highlight early involvement of the choroid plexus in central nervous system inflammation. ASN Neuro. 2013;5(1):e00110.
184. Ludwig A, et al. Rapid binding of electrostatically stabilized iron oxide nanoparticles to THP-1 monocytic cells via interaction with glycosaminoglycans. Basic Res Cardiol. 2013;108(2):328.
185. Tschoegl NW. The phenomenological theory of linear viscoelastic behavior. Berlin: Springer; 1989.
186. Fletcher DA, Mullins RD. Cell mechanics and the cytoskeleton. Nature. 2010;463(7280):485–92.
187. Plodinec M, et al. The nanomechanical signature of breast cancer. Nat Nanotechnol. 2012;7(11):757–65.
188. Jonietz E. Mechanics: the forces of cancer. Nature. 2012;491(7425):S56–7.
189. Fung Y. Biomechanics: mechanical properties of living tissue. New York: Springer-Verlag; 1993.
190. Fabry B, et al. Time scale and other invariants of integrative mechanical behavior in living cells. Phys Rev E Stat Nonlinear Soft Matter Phys. 2003;68(4 Pt 1):041914.
191. Lambert SA, et al. Bridging three orders of magnitude: multiple scattered waves sense fractal microscopic structures via dispersion. Phys Rev Lett. 2015;115(9):094301.
192. Ozawa H, et al. Comparison of spinal cord gray matter and white matter softness: measurement by pipette aspiration method. J Neurosurg. 2001;95(2 Suppl):221–4.
193. Guck J, et al. The optical stretcher: a novel laser tool to micromanipulate cells. Biophys J. 2001;81(2):767–84.
194. Tan K, et al. Characterising soft tissues under large amplitude oscillatory shear and combined loading. J Biomech. 2013;46(6):1060–6.
195. Kiss MZ, Varghese T, Hall TJ. Viscoelastic characterization of in vitro canine tissue. Phys Med Biol. 2004;49(18):4207–18.
196. Parker KJ. Experimental evaluations of the microchannel flow model. Phys Med Biol. 2015;60(11):4227–42.
197. Bilston LE, Thibault LE. The mechanical properties of the human cervical spinal cord in vitro. Ann Biomed Eng. 1996;24(1):67–74.
198. Samani A, Zubovits J, Plewes D. Elastic moduli of normal and pathological human breast tissues: an inversion-technique-based investigation of 169 samples. Phys Med Biol. 2007;52(6):1565–76.
199. Venkatesh SK, Yin M, Ehman RL. Magnetic resonance elastography of liver: technique, analysis, and clinical applications. J Magn Reson Imaging. 2013;37(3):544–55.
200. Othman SF, et al. Microscopic magnetic resonance elastography (microMRE). Magn Reson Med. 2005;54(3):605–15.
201. Urayama K, Kawamura T, Kohjiya S. Structure-mechanical property correlations of model siloxane elastomers with controlled network topology. Polymer. 2009;50(2):347–56.
202. Mendoza-Novelo B, et al. Decellularization of pericardial tissue and its impact on tensile viscoelasticity and glycosaminoglycan content. Acta Biomater. 2011;7(3):1241–8.

203. Al Jamal R, Roughley PJ, Ludwig MS. Effect of glycosaminoglycan degradation on lung tissue viscoelasticity. Am J Physiol Lung Cell Mol Physiol. 2001;280(2):L306–15.
204. Ipek-Ugay S, et al. Tabletop magnetic resonance elastography for the measurement of viscoelastic parameters of small tissue samples. J Magn Reson. 2015;251:13–8.
205. Tzschatzsch H, et al. Tomoelastography by multifrequency wave number recovery from time-harmonic propagating shear waves. Med Image Anal. 2016;30:1–10.
206. Hirsch S, Braun J, Sack I. Magnetic resonance elastography: physical background and medical applications. Weinheim: Wiley-VCH; 2017.